JGR Oceans

RESEARCH ARTICLE
10.1029/2018JC014814

Net Submarine Groundwater-Derived Dissolved Inorganic Nutrients and Carbon Input to the Oligotrophic Stratified Karstic Estuary of the Krka River (Adriatic Sea, Croatia)

Jianan Liu[1], Enis Hrustić[2,3], Jinzhou Du[1], Blaženka Gašparović[4], Milan Čanković[4], Neven Cukrov[4], Zhuoyi Zhu[1], and Ruifeng Zhang[1,5]

[1]State Key Laboratory of Estuarine and Coastal Research, East China Normal University, Shanghai, China, [2]Institute for Marine and Coastal Research, University of Dubrovnik, Dubrovnik, Croatia, [3]Center for Marine Research, Ruđer Bošković Institute, Rovinj, Croatia, [4]Division for Marine and Environmental Research, Ruđer Bošković Institute, Zagreb, Croatia, [5]Institute of Oceanology, Shanghai Jiao Tong University, Shanghai, China

Abstract Submarine groundwater discharge (SGD) is a significant source of biogenic elements in estuaries, and relevant studies in karstic estuaries are scarce. Krka River Estuary (KRE), located on the eastern Adriatic Sea (Croatia), is a typical oligotrophic stratified karstic estuary. In this study, based on ^{226}Ra and ^{228}Ra, the total SGD flux into the KRE surface layer was estimated to be (12.8–16.2) × 10^5 m^3/day. A conservative estimation of the fresh groundwater flux was (5.0–8.3) × 10^5 m^3/day, which accounts for 10–17% of the Krka River discharge into the estuary. By establishing water and nutrient budgets in the KRE surface layer, we found that SGD dominated the nutrient sources, although it accounted for a small portion of the total inflow water. Specifically, net SGD-derived dissolved inorganic nitrogen (DIN) and silicates contributed 58–90% and 24–64%, respectively, to the total input fluxes. These results indicate that SGD was a major external nutrient source, in which net SGD-derived high DIN flux and high DIN to dissolved inorganic phosphorus ratio may affect productivity in the KRE ecosystem and nearby Adriatic Sea. Additionally, net SGD-derived dissolved inorganic carbon (DIC) flux in the KRE (1.53 mol · m^2 · day) was much higher than those in most estuaries worldwide, suggesting that the DIC-enriched karst aquifers are important sources for global carbon cycle. Therefore, the impact of net SGD-derived DIC from karst aquifers on coastal seas will likely become more evident and substantial with further development of global climate change, such as sea level rise.

Plain Language Summary Coastal karst aquifers are very vulnerable and sensitive to climate and environmental changes. In this study, we evaluated the impacts of submarine groundwater discharge in a typical oligotrophic highly stratified karstic estuary. Using multiple parameters and mathematical models, we found that the net SGD-derived nutrient flux could affect the productivity of this coastal ecosystem, notably contributing to forming the conditions that lead to the occurrence of phytoplankton blooms. In addition, nutrient-enriched SGDs from the karst aquifers are likely to be important but easily ignored sources for the global carbon cycle. Taken together, our study revealed the impacts of submarine groundwater from the karst aquifers on the coastal seas, which shall become increasingly evident and substantial with further development of global climate change, such as the rise of sea level.

Key Points:
- ^{226}Ra and ^{228}Ra were used to estimate SGD in an oligotrophic stratified karstic estuary
- Net SGD-derived nutrients have potential to impact the ecosystem in the Krka River Estuary by high DIN flux and DIN:DIP ratio
- SGD from DIC-enriched coastal karst aquifers make a significant contribution to the carbon cycle of the coastal seas worldwide

Supporting Information:
- Supporting Information S1

Correspondence to:
J. Du,
jzdu@sklec.ecnu.edu.cn

Citation:
Liu, J., Hrustić, E., Du, J., Gašparović, B., Čanković, M., Cukrov, N., et al. (2019). Net submarine groundwater-derived dissolved inorganic nutrients and carbon input to the oligotrophic stratified karstic estuary of the Krka River (Adriatic Sea, Croatia). *Journal of Geophysical Research: Oceans*, *124*, 4334–4349. https://doi.org/10.1029/2018JC014814

Received 29 NOV 2018
Accepted 28 MAY 2019
Accepted article online 7 JUN 2019
Published online 28 JUN 2019

1. Introduction

An estuary is a critical zone connecting the mainland and adjacent sea, being the primary region where the continuous exchange of water and chemical components between land and sea/ocean occurs. There are numerous reports on the biogenic element processes in the estuaries/coasts and seas, for instance, on trace metals, nutrients, and carbon (Cai et al., 2004; Hatje et al., 2003; Kelly & Moran, 2002). Numerous studies have reported a significant transport of solutes via submarine groundwater discharge (SGD), which is defined as any and all flow of water on continental margins from the seabed to the coastal ocean, regardless of fluid composition or driving force, and generally happens in permeable geological material (submerged sediment) saturated with water (e.g., Burnett et al., 2003; Moore, 2010). The excess of SGD-derived biogenic elements, especially nutrients, has the potential to impact marine ecosystems, via significantly increasing concentrations of bioavailable nitrogen and phosphorus and changing N:P ratios, which may cause environmental problems, such as eutrophication, harmful algal blooms, and hypoxia (Lee et al., 2009; Li et al., 1999;

McCoy et al., 2011). In addition, previous studies have also shown that SGD can be the major source of dissolved inorganic carbon (DIC) in the estuaries (Moore et al., 2006; Sadat-Noori et al., 2016).

The ecosystem of the Krka River Estuary (KRE) is very sensitive to inputs of external substances because it is located in the area of the oligotrophic Adriatic Sea (the northernmost basin of the Mediterranean Sea; Zavatarelli et al., 1998; Šupraha et al., 2014). The KRE is a typical highly stratified karstic estuary characterized by low tidal impact in comparison to the river flow (Gržetić et al., 1991). Therefore, the Krka River significantly controls the depth of the sharp salinity gradient (halocline). A relatively thick (10–50 cm) halocline layer in the KRE is positioned between the depths of 2 and 5 m (Gržetić et al., 1991, and references therein). There is an organic film developed at the halocline (Žutić & Legović, 1987), enriched by dead freshwater phytoplankton and zooplankton fecal pellets (Ahel et al., 1996; Denant et al., 1991). Bacterial productivity (Fuks et al., 1991) and accumulation of pollutants (Ahel & Terzić, 2003) are more intense within the halocline than in more oligotrophic and unpolluted marine layer below the halocline. Thus, the halocline divides the water column of the KRE into two parts that are different from each other not only hydrologically but also chemically and biologically (Legović et al., 1994; Svensen et al., 2007; Žic & Branica, 2006). The Krka River belongs to the most pristine European rivers. The drainage basin of Krka River is very sparsely populated, and industrial development is limited. Additionally, input of clastic material of terrigenous origin in the Krka River Estuary is very small because of the number of tufa cascades along the Krka River stretching over tens of kilometers, which significantly reduces suspended material transport. Extremely low input of terrigenous material mainly comes from the anthropogenic sources near the city of Šibenik (Legović et al., 1991, 1994; Svensen et al., 2007). Because of its unique biological and geological characteristics, the lower part of the river region is protected as the Krka National Park. Although numerous studies have described the ecosystem of the KRE (e.g., Cetinić et al., 2006; Viličić et al., 1989), there are no reports on the importance of SGD as nutrient and DIC source for the Krka River, its estuary, and the regions of the coastal Adriatic Sea under their direct influence. Gržetić et al. (1991) mentioned groundwater springs in the upper KRE without evaluating their influence, while Cauwet (1991) reported on the DIC in the Krka River, but not in the SGD entering the KRE. Many studies dealt with SGD and its derived materials in the Mediterranean Sea regions, but only a few of them are related to DIC (Garcia-Solsona, Garcia-Orellana, Masqué, Garces, et al., 2010; Rodellas et al., 2015). Therefore, it is necessary to evaluate the significance of SGD in transporting DIC in order to fill the gap in modeling the predictions of DIC flux from total freshwater sources to coastal seas via karstic stratified estuaries, taking into account the trend of sea level rise and its intrusion into the karst aquifers (Cao et al., 2016; Ketabchi et al., 2016).

Naturally occurring radioactive isotopes have been widely used as tracers in evaluating SGD in coastal waters, especially radon and radium isotopes (^{223}Ra, ^{224}Ra, ^{226}Ra, and ^{228}Ra; Burnett et al., 2006; Moore et al., 2006). Therefore, in this study, samples for Ra isotope, nutrient, and DIC analyses were collected along the salinity gradient in the Krka River and its estuary. We focused on understanding the importance of SGD in the KRE, not only in water balance but also in SGD-derived nutrients and DIC that may affect the nutrient budgets and, consequently, microbial food web interactions and overall productivity of the study area. Given that karstic stratified estuaries are distributed along the eastern coast of the Adriatic Sea, and similar systems exist in the Mediterranean (e.g., Garcia-Solsona, Garcia-Orellana, Masqué, Rodellas, et al., 2010; Rodellas et al., 2017) and worldwide (e.g., Gonneea et al., 2014; McCormack et al., 2014), our findings provide new information and a valuable example for calculating DIC budgets in the coastal zones with karst aquifers worldwide.

2. Materials and Methods

2.1. Study Area

The Krka River is a typical groundwater-fed karstic river that is located on the eastern coast of the Adriatic Sea (Croatia; Figure 1a). The measured Krka River flow is between 5 and 565 m^3/s with an average annual flow between 40 and 60 m^3/s (Bonacci et al., 2006). Its hydrogeological drainage area covers approximately 2,427 km^2 with a length of 49 km for the freshwater section (Figure 1b), while the whole estuary extends for an additional 24 km and usually refers to the area between stations KR1 and KR10 (Figures 1c and 1d). The KRE was formed during the Holocene transgression and contains a fresh-brackish surface layer moving seaward and a bottom seawater layer as a countercurrent, moving upward (Cukrov et al., 2009). During winter,

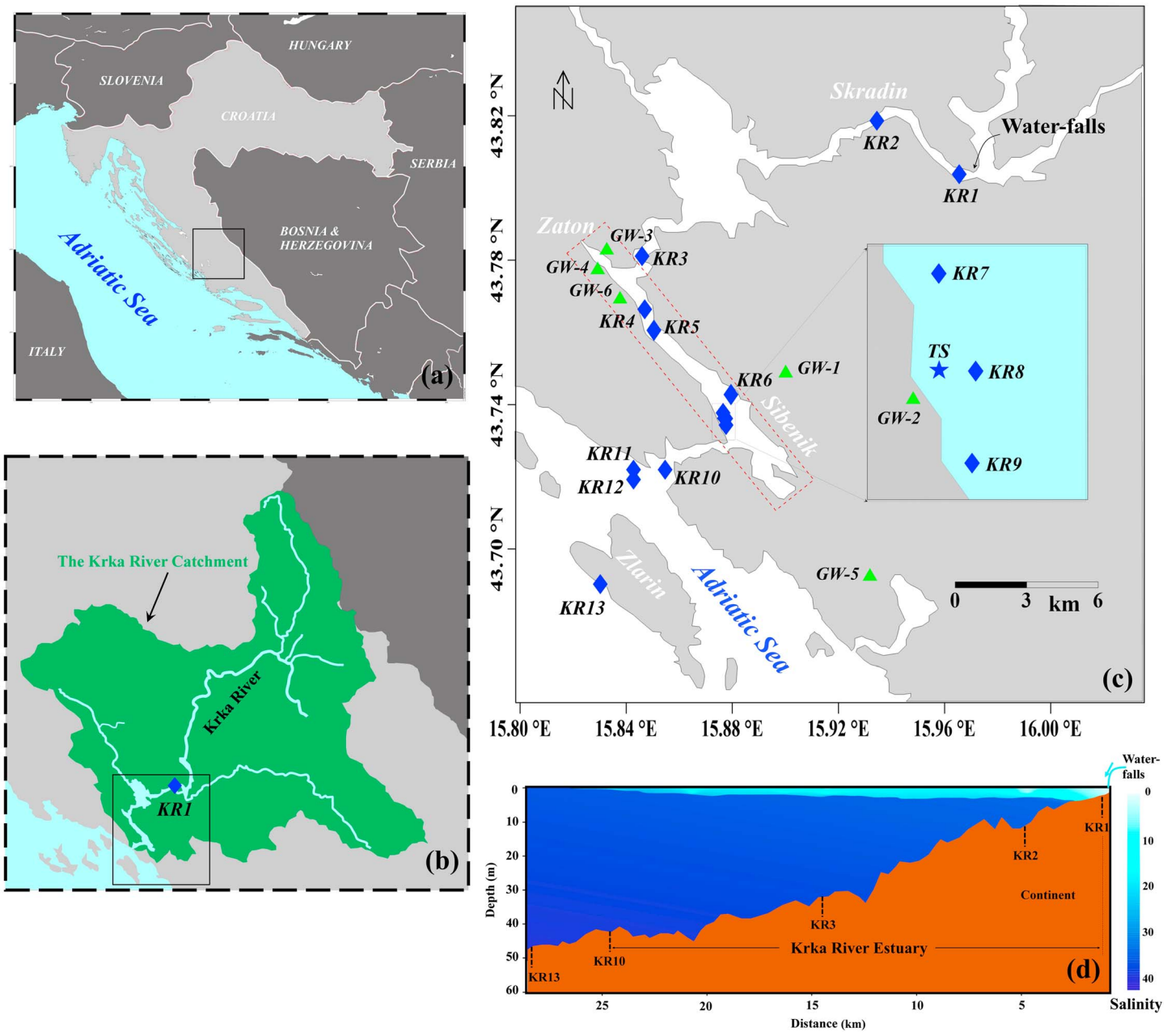

Figure 1. Sampling locations in the Krka River and its estuary. (a) Location of the Krka River, (b) the Krka River catchment, and (c) distribution of the sampling stations; blue diamonds represent regular sampling stations within the Krka Estuary and the nearby coastal sea (modified from Cukrov et al., 2008), green triangles represent sampling stations for groundwater, blue pentagram represents the station for time series observation, and red dashed box represents the specific study area for estimating SGD. (d) Schematic diagram of the whole KRE; the color bar represents the salinity variation in the vertical profile.

the flushing time is between 6 and 20 days for the brackish water above the halocline in the whole KRE, whereas flushing time in the marine water layer below halocline is between 50 and 100 days. During summer, the flushing time above the halocline in the whole KRE is up to 80 days, whereas flushing time in marine water is up to 250 days (Legović, 1991). The KRE is characterized by relatively low tidal range of no more than 0.5 m (Žic and Branica, 2006). Therefore, the Krka River plays a dominant role in controlling water quality and permanent vertical stratification in the estuary (Cukrov et al., 2012; Legović et al., 1994). Numerous submerged or ephemeral springs occur along the Krka River (Cukrov et al., 2012; Kniewald et al., 2006), as one type of submarine groundwater, and they have the potential to affect the ecosystem by transporting their associated substances into the estuary. Due to the rising intensity of

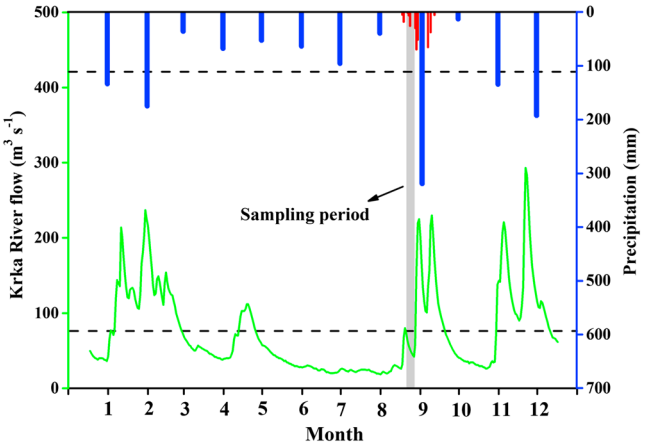

Figure 2. The Krka River flow and cumulative monthly precipitation in the city of Šibenik in 2014. Red bars represent daily precipitation in September 2014. The black dashed lines represent the average Krka River flow and monthly precipitation in 2014. Data are from Šibenik meteo organization (http://www.sibenik-meteo.com).

anthropogenic activities, subtle changes have occurred in the ecosystem of the Krka River and its estuary (Cukrov et al., 2008; Kwokal et al., 2002).

2.2. Sampling Strategy

A field survey was performed in the Krka River and its estuary during the period of 4–10 September 2014. At that time, the average Krka River flow was approximately 56 m^3/s (Figure 2). The sampling area covered transects from the lowest stream of the Krka River (KR1) via the estuary (KR2-KR10) to the open seawater outside the estuary (KR11-KR13; Figure 1). Samples of surface waters were collected directly from a depth of approximately 0–0.5 m using Niskin bottles of 5 L to fill the container with 60 L per sample. In the KRE, we also conducted a continuous 24-hr time series observation over one complete tidal cycle by sampling the surface water of 0–0.5 m at the time series (TS) station every 3 hr (Figure 1). This method has been widely used to evaluate the SGD (Garcia-Orellana et al., 2010; Peterson et al., 2008; Wang & Du, 2016). Groundwater samples were collected in springs and wells along the KRE. In addition, corresponding water samples for nutrients and DIC analyses were collected with polyethylene bottles at these stations. At the KR3 station, we collected nutrient samples across the vertical profile at depths of 0.5, 1, 2, 6, and 12 m. Salinity, temperature, and dissolved oxygen (DO) at all stations were determined in situ using a multiparametric probe (Hach Lange HQ40D).

2.3. Measurements of Ra Isotopes, Dissolved Inorganic Nutrients, and Carbon

After removing the suspended sediments by filtration cartridges (pore size of 0.5 μm), the water samples for Ra isotopes measurements were passed through a column filled with approximately 20-g MnO_2-impregnated acrylic fiber at a flow rate of ~0.5 L/min. Ra isotopes ^{228}Ra and ^{226}Ra were determined by HPGe gamma spectrometry (Ortec, GWL-120-15-XLB-AWT), and the detector was calibrated using certified reference materials (batch number: 08121) obtained from the National Institute of Metrology, China, to ensure its accuracy (Liu et al., 2017; Wang et al., 2014). After leached from the MnO_2-impregnated acrylic fiber, Ra isotopes were coprecipitated with barium sulfate, and the precipitate was sealed for more than 20 days before measurements. The counting time for each sample was 24 to 48 hr. ^{226}Ra activities were measured using ^{214}Pb (295 and 352 keV) and ^{214}Bi (609 keV) peaks; ^{228}Ra activity was measured using ^{228}Ac (338- and 911-keV peaks). The uncertainties of ^{226}Ra and ^{228}Ra were 3.6–12% and 2.8–15%, respectively.

Samples (50 ml) for analysis of ammonium (NH_4^+) were stabilized by addition of 2 ml phenol (1 mol/L, dissolved in 95% ethanol; Ivančić & Degobbis, 1984) and stored in the dark at 4 °C. Samples (500 ml) for other nutrients were stored at −22 °C. The concentrations of nitrate (NO_3^-), nitrite (NO_2^-), NH_4^+, reactive orthosilicates (SiO_4^{4-}, hereafter termed DSi), and orthophosphate (PO_4^{3-}, hereafter termed dissolved inorganic phosphorus, i.e., DIP) were determined as described in Strickland and Parsons (1972) and Grasshoff et al. (2009) by using a spectrophotometer (PerkinElmer Lambda15) combining 1- and 10-cm cuvettes, as needed. The detection limits and reproducibility for the nutrients were as follows: 0.05 and 0.025 μmol/L for NO_3^-, 0.01 and 0.01 μmol/L for NO_2^-, 0.1 and 0.098 μmol/L for NH_4^+, 0.1 and 0.06 μmol/L for SiO_4^{4-}, and 0.03 and 0.03 μmol/L for DIP. The concentration of DIN equals the sum of NO_2^-, NO_3^-, and NH_4^+ concentrations.

DIC concentrations were determined using TOC-V Analyser (Shimadzu®), which was calibrated using a mix of sodium carbonate and sodium bicarbonate. Briefly, 100-μL sample was injected in a reactor containing H_3PO_4 25% (w/w; analytical reagent grade), DIC was converted into CO_2, then volatilized by sparging and detected by nondispersive infrared detector. The limit of detection was 0.008 mmol CO_2 per liter.

3. Results

3.1. Hydrological Features

During the investigated period, salinity in the surface water of the lower stream of the Krka River and its estuary ranged from 0.2 at station KR1 to 33.3 at station KR10 (Table 1). Freshwater affected only the upper ~2.5-

Table 1
Activities of ^{226}Ra and ^{228}Ra and Concentrations of Nutrients in the Krka River and Its Estuary

	Depth		^{226}Ra	Error	^{228}Ra	Error	$^{228}Ra/^{226}Ra$	DIN	PO_4^{3-}	SiO_4^{4-}	DIC
Sample	m	Salinity	dpm/m^3				ratio	μmol/L			mmol/L
Surface water											
KR1	0–0.5	0.2	90	5	33	4	0.4	4.63	0.27	31.0	13.6
KR2	0–0.5	2.3	90	5	61	8	0.7	4.16	0.54	26.9	13.3
KR3	0–0.5	7.1	86	5	57	7	0.7	5.40	0.69	32.9	13.0
KR4	0–0.5	11.2	101	5	102	7	1.0	5.81	0.24	25.8	12.2
KR5	0–0.5	12.1	121	7	118	10	1.0	na	na	na	na
KR6	0–0.5	12.2	92	8	107	7	1.2	na	na	na	na
KR7	0–0.5	20	116	5	102	6	0.9	na	na	na	na
KR8	0–0.5	14.9	92	5	126	6	1.4	4.75	0.33	22.4	11.9
KR9	0–0.5	19	116	5	115	7	1.0	na	na	na	na
KR10	0–0.5	21.7	130	5	127	7	1.0	2.96	0.24	13.4	10.8
KR11	0–0.5	27.1	110	5	82	8	0.7	2.10	0.21	8.61	10.2
KR12	0–0.5	33.3	103	5	86	8	0.8	1.89	0.25	6.29	9.2
KR13	0–0.5	36.9	107	5	49	8	0.5	1.00	0.25	3.36	8.7
Groundwater											
GW-1	0.5	3.8	209	15	347	8	1.7	67.53	0.67	na	na
GW-2	0.5	3.4	189	11	281	20	1.5	80.18	0.23	120	13.2
GW-3	0.2	1.1	156	19	206	23	1.3	179.91	0.95	na	18.7
GW-4	0.2	0.2	105	9	205	14	2.0	na	na	na	17.7
GW-5	0.2	10.1	na	na	na	na	na	150.00	0.52	na	na
GW-6	0.2	22.4	na	na	na	na	na	152.00	0.47	na	na
Time-series observation											
TS-1	0–0.5	11.6	102	5	63	8	0.6	5.77	0.23	31.1	12.7
TS-2	0–0.5	14.0	108	5	84	8	0.8	3.88	0.24	23.6	12.1
TS-3	0–0.5	13.9	103	5	91	8	0.9	4.09	0.39	23.2	12.1
TS-4	0–0.5	13.2	91	5	96	6	1.1	3.56	0.39	27.9	12.3
TS-5	0–0.5	12.3	116	5	119	7	1.0	3.97	0.31	29.9	12.7
TS-6	0–0.5	11.0	106	5	79	8	0.7	4.09	0.36	28.6	12.8
TS-7	0–0.5	11.0	114	5	81	8	0.7	6.57	0.31	26.9	12.7
TS-8	0–0.5	11.2	119	5	139	7	1.2	3.09	0.33	30.5	12.4
TS-9	0–0.5	10.7	93	5	76	7	0.8	4.69	0.59	32.0	12.5

na: not analyzed
Note. KR1 is the riverine station, KR2-KR10 are in the KRE, and KR11-KR13 are seawater stations outside KRE.

m layer, the thickness of which decreased seaward (supporting information Figure S1a). The temperature and DO ranged from 18.5 to 28.7 °C and from 6.73 to 10.60 mg/L, respectively. Maxima of both were detected at the bottom of halocline lengthwise the estuary. The distribution of subsurface temperature maxima is a consequence of the passage of solar radiation through the transparent brackish water and slow entrainment in the seawater (Legović et al., 1991, 1994). In the vertical profiles, temperature and DO decrease gradually from the halocline (~2.5 m) toward the bottom water (Figures S1b, S1c, and S2a). In the water column of the KRE, phytoplankton has the highest abundances above and within the halocline due to its strong density gradient and relatively high concentration of nutrients (Cetinić et al., 2006). With sufficient nutrients in the fresh and brackish water, the phytoplankton community can produce more oxygen and organic matter above and within the halocline layer (Cota et al., 1996).

3.2. Dissolved Nutrients and DIC in the KRE

In the surface water of the Krka River and the KRE, nutrient concentrations (μmol/L) ranged from 1.00 to 5.81 for DIN, 0.21 to 0.69 for DIP, and 3.36 to 32.92 for DSi, while DIC ranged from 8.71 to 13.63 mmol/L (Table 1). Concentrations of DIN, DSi, and DIC decreased from upper stream toward the mouth of estuary and had significant negative correlations with salinity ($r = -0.86$, $p < 0.01$ for DIN, $r = -0.96$, $p < 0.001$ for DSi, and $r = -0.99$, $p < 0.001$ for DIC) (Figures 3a, 3c, 3e, and 3f). There was no significant correlation between DIP concentrations and salinity ($r = -0.55$, $p = 0.064$; Figures 3a and 3d). The groundwater around the KRE had significantly higher DIN and DSi but similar DIP compared to the Krka River and KRE surface water (Table 1). DIN/DIP ratios in the surface water at most stations were below the Redfield ratio of 16

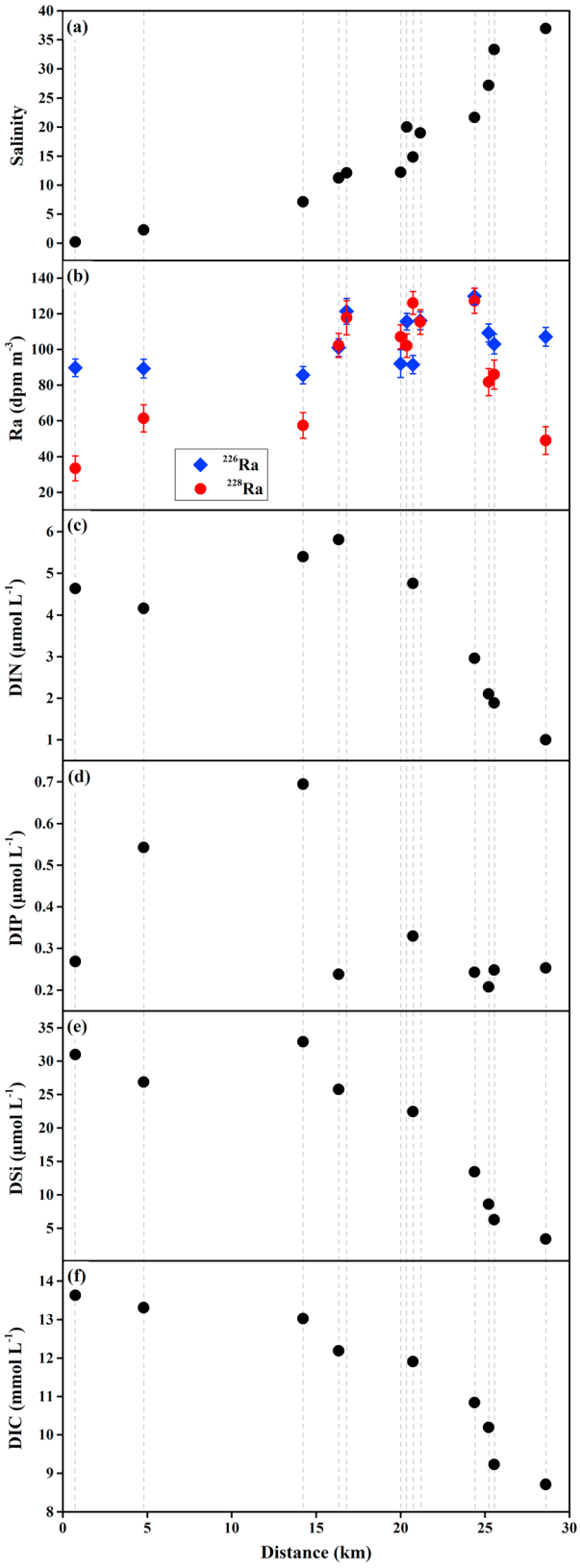

Figure 3. (a) salinity, (b) Ra activities, (c–e) nutrients, and (f) DIC in the surface water along the KRE. The *X* axis represents the distance from the end-member of freshwater.

(Redfield et al., 1963), indicating a potential lack of nitrogen for the balanced growth of phytoplankton. DIN, DSi, and DIC concentrations were all comparatively high above the halocline and low below the halocline (the presented case from station KR3; Figure S2b), suggesting that the DIN, DSi, and DIC below the halocline do not have a significant potential to affect the surface estuarine water. In comparison, DIP showed a different pattern with the maximum value in the surface water, the minimum value near the halocline, and relatively high values below the halocline (Figure S2).

3.3. Dissolved Ra Isotopes in the KRE

The dissolved ^{226}Ra and ^{228}Ra activities during the sampling period ranged from 86 to 130 dpm/m^3 and from 33 to 127 dpm/m^3, respectively (Figure 3b and Table 1). Ra activities were low in fresher waters in the upper KRE, reaching the highest values in the middle region of the KRE, and then declined outside the estuary (Figure 3b). In the groundwater around the KRE, ^{226}Ra and ^{228}Ra activities ranged from 105 to 209 dpm/m^3 and from 205 to 347 dpm/m^3, with averages of 165 and 260 dpm/m^3, respectively. ^{228}Ra activities in groundwater were significantly higher than those in the Krka River and its estuary, whereas there was no statistically significant difference for ^{226}Ra between groundwater and KRE surface water.

3.4. Time Series Observation

The results from 24-hr time series observation demonstrated that all the key measured variables changed over the tidal cycle, even though the range of tidal height was only approximately 0.4 m. Salinity varied with the water depth and was driven by the tide. Maximum (14.0) and minimum (10.7) salinities were found at high and low tides, respectively (Figure 4a and Table 1). The ^{226}Ra activities over the time series observation ranged from 91 to 119 dpm/m^3 with an average of 106 ± 15 dpm/m^3 (n = 9), and ^{228}Ra activities ranged from 63 to 139 dpm/m^3 with an average of 92 ± 22 dpm/m^3 (n = 9). Nutrient concentrations also varied with the salinity changes during the time series observation (Figure 4e). DIP and DSi concentrations had apparent opposite trends to water depth with a small hysteresis effect observed. However, correlation analysis did not give statistically significant correlation between the nutrients and salinity (r = −0.44, p = 0.123 for DIP; r = −0.43, p = 0.147 for DSi; and r = 0.16, p = 0.341 for DIN). Overall, Ra activity and nutrient concentrations varied over the time series observation due to different material sources, including those from open seawater, river water, and the SGD, but there were no statistically significant correlations between nutrient concentrations and Ra activity.

For DIC, the concentration varied within a narrow range from 12.1 to 12.8 mmol/L, with an average of 12.5 mmol/L, and showed a significant opposite trend to the water depth. Namely, high DIC concentration corresponded to low water depth and vice versa (Figure 4d). Unlike nutrients, there was no hysteresis observed for DIC.

4. Discussion

4.1. Ra Isotopes

In our study, the measured ^{226}Ra activities were similar to those reported for some riverine systems in Croatia and worldwide, whereas ^{228}Ra

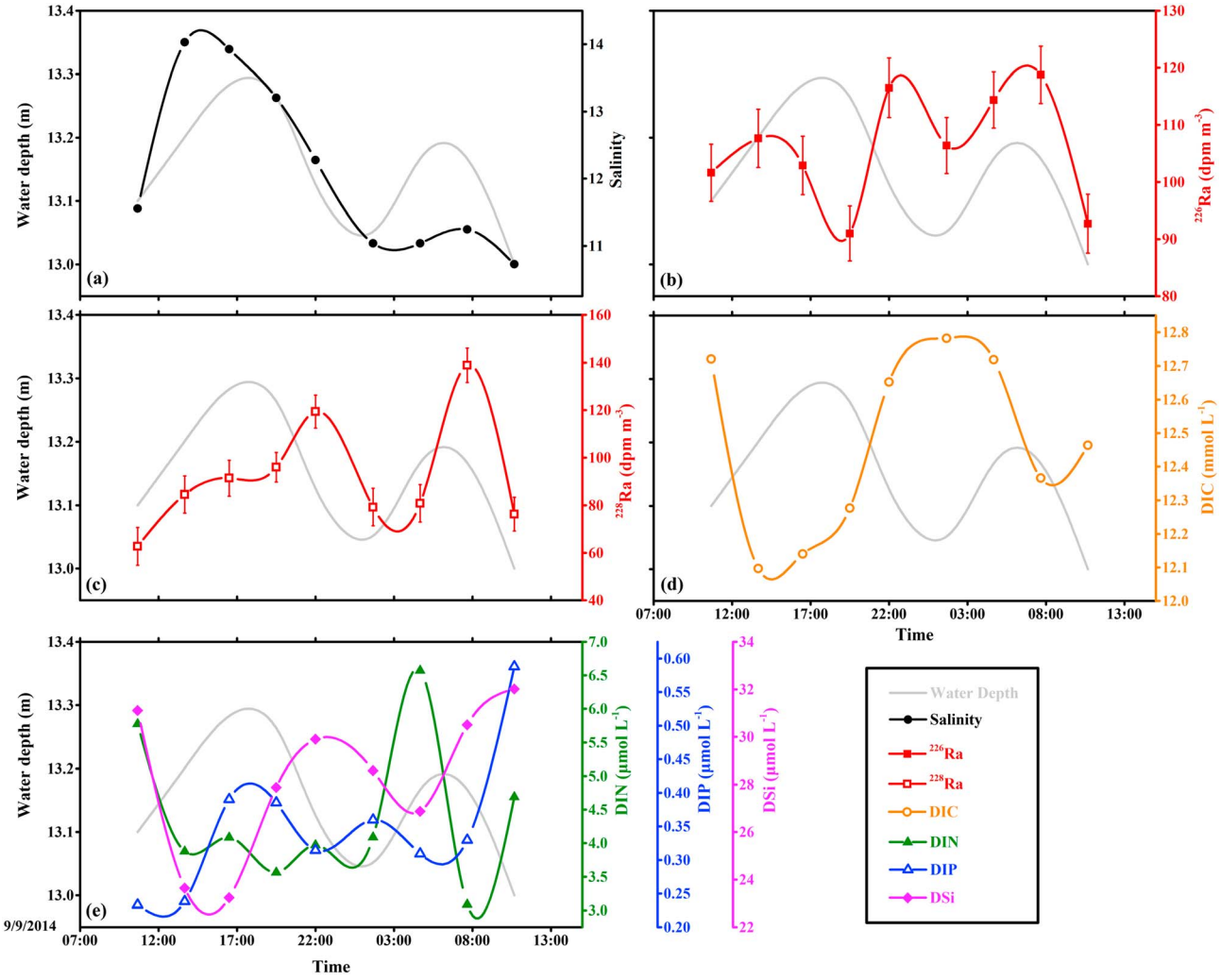

Figure 4. Variations between water depth and (a) salinity, (b) ^{226}Ra activity, (c) ^{228}Ra activity, (d) DIC, and (e) nutrient concentrations in the surface water of the KRE during the time series observation.

activities were lower compared to some riverine systems in Croatia and worldwide (Bituh et al., 2008; Krest & Moore, 1999; Su et al., 2015). This phenomenon might be caused by the carbonate sedimentation that prevails in this karstic river system, resulting in more enriched uranium-238 (^{238}U, a parent nuclide of ^{226}Ra) than thorium-232 (^{232}Th, a parent nuclide of ^{228}Ra; Cukrov & Barišić, 2006; Cukrov et al., 2009). Due to the existence of halocline in the KRE, similar to nutrient and DIC, it is not likely that Ra desorption from sediments could support the Ra activity in the KRE surface layer. Besides, because of the numerous tufa barriers and the big lake in the freshwater part preceding the estuary (serving as traps for the particles), the level of suspended matter introduced by the river is very low, ranging between 0.4 and 6.0 g/m^3 (Cindrić et al., 2015). We employed the value of 6 g/m^3, as explained in S2 in the supporting information. Since the desorbed Ra activities from suspended matter were neglectable compared to the activities in the KRE water, the significant increase in Ra activities after 15 km from the freshwater end-member was likely under the considerable influence of SGD along the coast. Indeed, there are several underground springs that flow out into the KRE, especially in the bay near Zaton village located in the lower part of the estuary (Bonacci, 1995; Cukrov et al., 2012). Those underground springs may contribute to the higher Ra activities obtained at stations KR4-KR9.

During the 24-hr time series observation, we did not obtain significant correlations between Ra activities and water depth variation (Figures 4b and 4c). This could be explained, at least in part, by the much smaller tidal

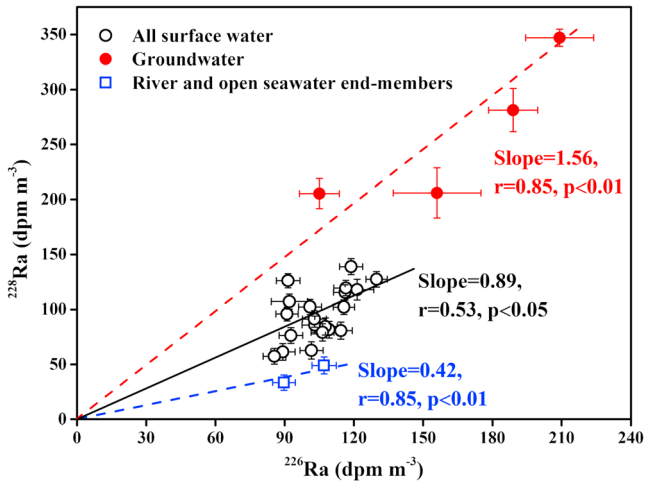

Figure 5. Activities of ^{228}Ra versus ^{226}Ra in all the KRE surface water sampling stations and their surrounding groundwater.

changes in the KRE than in other regions around the world, where Ra activities and water depth variation showed a significant correlation (Garcia-Orellana et al., 2010; Sadat-Noori et al., 2015; Wang & Du, 2016). During the high tide, the stronger intrusion of the open seawater reduced the influence from submarine springs with high Ra activity. However, because the TS station was close to the coast, more Ra could come from recirculated seawater, and vice versa, resulting in the lack of typical trends between Ra activities and water depth. These results also indicate that Ra activities in our study area were probably under the influences of submarine fresh groundwater and recirculated seawater.

4.2. Ratios of Ra Isotopes

Generally, even that the geochemical behaviors of ^{226}Ra and ^{228}Ra should be the same, there are differences between the rates of their production from their parent nuclides because of their different half-lives. Therefore, variable ^{228}Ra/^{226}Ra activity ratios point to different sources of Ra isotopes. From the Krka River to the estuary region, ^{228}Ra/^{226}Ra activity ratios increased from 0.4 to 1.4, especially in the KRE the ratios varied between 0.9 and 1.4. In comparison, ^{228}Ra/^{226}Ra activity ratios in groundwater were around 1.3–2.0 (Table 1), indicating the significant influence of groundwater on the KRE. In addition, groundwater samples had an approximately linear relation between ^{228}Ra and ^{226}Ra activities with a regression slope of 1.56 ($r = 0.85$, $p < 0.01$), which was higher than the slope of 0.89 for the surface waters ($r = 0.53$, $p < 0.05$) and regression slope (slope = 0.42, $r = 0.85$, $p < 0.01$) of expected conservative mixing between Krka River freshwater and open seawater (Figure 5). These results indicate that the sampled groundwater could be the proper source for Ra in the KRE surface water (Wang et al., 2018).

4.3. Estimation of SGD

Generally, SGD includes two components, fresh groundwater and recirculated groundwater where seawater infiltrates into the aquifer. We employed three end-members mixing model and Ra mass balance model to estimate the SGD flux into the KRE surface layer (Gu et al., 2012; Moore, 1996, 2003, 2010; Moore et al., 2008; Sanford et al., 1992; see details in supporting information S1 and S2). By using three end-member mixing model, we calculated SGD flux to be (6.5–26.7) $\times 10^5$ m^3/day, with an average of 16.2 $\times 10^5$ m^3/day. In comparison, Ra mass balance model gave estimated SGD flux of (4.7–21.0) $\times 10^5$ m^3/day, with an average of 12.8 $\times 10^5$ m^3/day. These approaches showed similar results, and both contain two SGD components. Additionally, we evaluated the effects of tidal pumping on SGD by time series observation in a tidal cycle, resulting in a range of (3.2–18.1) $\times 10^5$ m^3/day with an average of 7.8 $\times 10^5$ m^3/day (see details in supporting information S3). From these calculations, we can conclude that tidal-driven SGD accounts for approximately 49–61% of the total SGD flux, suggesting the importance of tidal pumping in driving SGD flux albeit the tidal range is very small in the KRE surface layer. It should be noted that majority of the SGD flux estimated in a tidal cycle could represent recirculated groundwater, which was derived from tidal and waves pumping (Burnett et al., 2006; Ji et al., 2013; Moore, 2010; Wang & Du, 2016), and to some extent affect terrestrial hydraulic gradients that drive fresh groundwater. Therefore, we considered the result of estimated SGD flux from time series observation as the recirculated groundwater discharge, which could represent a conservative flux of fresh groundwater discharge of (5.0–8.3) $\times 10^5$ m^3/day with an average of 6.6 $\times 10^5$ m^3/day. Then, the fresh groundwater would account for 41–52% of the total SGD and 10–17% of the Krka River discharge into the KRE surface waters during the sampling period. By comparing with other studies in the Mediterranean region (Table 2), we can conclude that the estimated SGD flux in our study is comparable to other reports.

In this study, we used the highest ^{228}Ra activity in groundwater in order to avoid potential overestimation of SGD. Even though a narrow range of ^{228}Ra activities in groundwater was observed, the total SGD and SFGD fluxes would increase by 36–38 and 34–39, respectively, if we used the average ^{228}Ra activity. Additionally, a variation of 1 day in flushing time could cause changes of 25–35% and 14–50 in total SGD and SFGD fluxes estimation, respectively. Except for these two sources, the uncertainties from the Krka River input and

Table 2
Comparison of SGD Fluxes in the Mediterranean

Region	Tracer	SGD ($m^3 \cdot m^2 \cdot day$)	Percentage to river	Reference
Balearic Islands, Spain	^{223,224,226,228}Ra	0.025 ± 0.007	na	Garcia-Solsona, Garcia-Orellana, Masqué, Garces, et al. (2010)
Castelló, Spain	^{223,224,226,228}Ra	0.055–0.089	na	Garcia-Solsona, Garcia-Orellana, Masqué, Rodellas, et al. (2010)
Dor Beach, Israel	^{222}Rn	7.1 *	na	Swarzenski et al. (2006)
Mar Menor, Spain	^{222}Rn	0.0008–0.0046	390–2,100%	Baudron et al. (2015)
	^{224}Ra	0.0093–0.040	4,300–18,600%	
La Palme lagoon, France	^{222}Rn	0.0076–0.040	na	Stieglitz et al. (2013)
	^{223,224}Ra	0.011–0.032	na	Bejannin et al. (2017)
	^{224}Ra	0.013 ± 0.0095	na	Tamborski et al. (2018)
Messiniakos Gulf, Greece	^{222}Rn	0.0042–0.028	4–20%	Pavlidou et al. (2014)
Donnalucata, Italy	^{226}Ra	10^3 *	na	Moore (2006)
	^{222}Rn	34–210 *	na	Burnett and Dulaiova (2006)
Lesina Lagoon, Italy	^{224}Ra	0.018–0.021	350–500%	Rapaglia et al. (2012)
Venice Lagoon, Italy	^{223,224,226,228}Ra	0.060–0.082	970–1,300%	Rapaglia et al. (2010)
Palma Beach, Spain	^{226,228}Ra	11.2 ± 2.6 *	na	Rodellas et al. (2014)
Gulf of Lion, France	^{226,228}Ra	0.00043–0.0084	1.6–29%	Ollivier et al. (2008)
Marina Lagoon, Egypt	^{222}Rn	0.021–0.060	na	El-Gamal et al. (2012)
Mediterranean Sea	^{228}Ra	0.0057–0.042	100–1,600%	Rodellas et al. (2015)
Upper KRE, Croatia	^{228}Ra	0.050–0.29	9.6–55%	This study

*units in $m^3 \cdot m \cdot day$
na: not available

mixing with Adriatic seawater played minor roles in estimating SGD flux, which resulted in total SGD uncertainties of 5.8–8.1% and 4.0–7.0% and SFGD uncertainties of 6.7–9.6% and 6.1–11%, respectively. Therefore, uncertainty analysis showed that the estimation of SGD in this study is mainly sensitive to the groundwater ^{228}Ra end-member choosing and the calculation of flushing time. Besides, Ra activity in the groundwater end-member may vary with time and seasons (Cerdà-Domènech et al., 2017), but we did not evaluate the temporal variability in Ra activity of the groundwater, in this way the estimated SGD fluxes usually represent the average values during the sampling period or even longer period. So, in order to reduce the error caused by ^{228}Ra activity variability in the groundwater end-member, we chose the highest ^{228}Ra activity in groundwater to obtain SGD fluxes.

4.4. Water Budget in the KRE Surface Layer

In addition, we used the method by X. Wang, Li, et al. (2015) to evaluate water mass balance in the KRE surface layer, with the assumption that the study area was a single box at a steady state. The conceptual water mass balance for the KRE surface layer is presented in Figure 6. The total water inflow should result from precipitation (Q_P) and freshwater discharge, including the total river flux (Q_R), wastewater (Q_W), and fresh groundwater discharge Q_{SFGD}. The water outputs include residual flow (Q_O) out of the KRE surface layer to the Adriatic Sea and evaporation (Q_E). Thus, the total water inflow equals the water outflow, and the water mass balance can be written as follows:

$$Q_R + Q_P + Q_W + Q_{SFGD} = Q_E + Q_O \quad (1)$$

The precipitation and evaporation fluxes for the analyzed section of the KRE during the sampling period were 45.3×10^5 and 30.5×10^5 m^3/day, respectively (data from http://www.esrl.noaa.gov/). The wastewater that spreads out from the city of Šibenik had an average outflow of approximately 0.046×10^5 m^3/day (data from http://www.wte.de/WTE-Group.aspx). Then, based on equation ((1)), the residual flow out of the KRE surface layer was estimated to be 69.9×10^5 m^3/day. From the water mass balance (Figure 6), we observed that the SGD contribution to the total water inflow was very small, ranging from 5.0 to 8.3%. In contrast, the contribution from the Krka River was at least 48%, which was the largest single component. Further, the water exchange flow, that is, mixing flow between the KRE surface layer and the coastal sea (Q_M), can be derived based on the salt balance using the following equation:

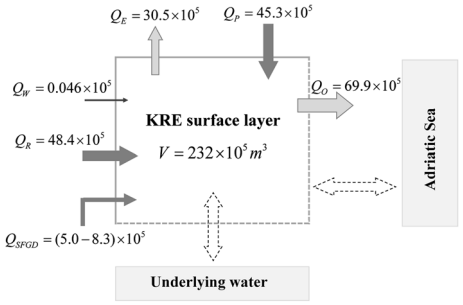

Figure 6. Water balance (m^3/day) in the KRE surface layer. The average SGD flux from the three methods was used to establish the water balance in the KRE.

$$Q_M(S_2-S_1) = Q_O(S_1+S_2)/2 \quad (2)$$

where S_1 (18.2) and S_2 (36.9) represent the mean salinities of the KRE surface layer and the Adriatic Sea, respectively. We estimated the water mixing flow to be 103×10^5 m^3/day, which included mixing flow out of the estuary and exchange with the underlying water below the halocline.

4.5. Net SGD-Derived Nutrient Fluxes to the KRE Surface Layer

Nutrients in the KRE were discussed extensively in relation to the freshwater inflow of the Krka River and anthropogenic sources from the city of Šibenik (Gržetić et al., 1991; Legović et al., 1991; Svensen et al., 2007). Here, we have determined that the Krka River contributed 22.4×10^3 mol DIN per day, 1.3×10^3 mol DIP per day, and 150×10^3 mol DSi per day to the analyzed section of the estuary during the sampling period (Figure 7). This has been calculated via multiplication of the Krka River freshwater discharge by nutrient concentrations in freshwater end-member. SGD-derived nutrients have been shown to be a major component and indisputable source in some estuarine systems (Liu et al., 2018; Rengarajan & Sarma, 2015; Su et al., 2011). The estimation of net export SGD nutrient fluxes could be derived from the difference between total SGD-associated nutrient fluxes and the return fluxes from the KRE surface layer to the groundwater (G. Z. Wang, Wang, et al., 2015). In this study, the total SGD-associated nutrient fluxes were calculated by multiplying the total SGD flux by its nutrient concentrations (126, 0.57, and 120 μmol/L for DIN, DIP, and DSi, respectively). The flux from the KRE to the groundwater was calculated by multiplying the recirculated groundwater flux by nutrient concentrations in the KRE surface layer (4.57, 0.34, and 27 μmol/L for DIN, DIP, and DSi, respectively). Therefore, the net SGD-derived nutrient fluxes to the KRE surface layer were estimated to be $(50.4–328) \times 10^3$, $(0.16–0.91) \times 10^3$, and $(47.0–270) \times 10^3$ mol/day for DIN, DIP, and DSi, respectively. These fluxes were equivalent to 225–1627%, 12–258%, and 31–281% of the riverine inputs to the KRE surface layer for DIN, DIP, and DSi, respectively. It seems that SGD provides a substantial contribution to DIN, DIP, and DSi loadings to the surface water of the KRE.

Similar to the water balance, we were able to establish nutrient budgets in the KRE surface layer based on a box model devised by Land Ocean Interactions in the Coastal Zone, assuming that the study was conducted at a steady state (Gordon et al., 1996). This model has been widely used to evaluate the relative importance of external nutrient inputs versus the physical transports and internal biogeochemical processes within a body of water (Liu et al., 2009, 2011; Wang & Du, 2016). In addition to riverine and SGD inputs, atmospheric deposition and wastewater were the other two sources for nutrient input to the KRE surface layer. Nutrient input from atmospheric deposition can be estimated by multiplying the atmospheric deposition rate by the surface area (Markaki et al., 2010; Rodellas et al., 2015), while nutrient input from wastewater can be estimated by multiplying wastewater nutrient concentrations by the wastewater flux (Gunes et al., 2012; Powley et al., 2016). In terms of nutrient outputs in this model, the net residual flux had a significant role. It can be estimated as $Q_O \times (C_1+C_2)/2$, where C_1 and C_2 are the nutrient concentrations in the KRE surface layer and the open seawater, respectively. Another term of nutrient fluxes out of the lower Krka estuary is the exchange with the open seawater, which was calculated here as $Q_M \times (C_1 - C_2)$. Therefore, based on the above results of each nutrient flux, the nutrient budgets in the KRE surface layer are shown in Figure 7. We found that DIN and DIP inputs were greater than their outputs, while DSi input was less than its output, indicating that the KRE surface layer system was a DIN and DIP sink and DSi source. SGD was the dominant source of DIN and DSi, which contributed 58–90% and 24–64% to the total DIN and DSi fluxes, respectively, into the KRE surface layer, followed by the Krka River and wastewater source.

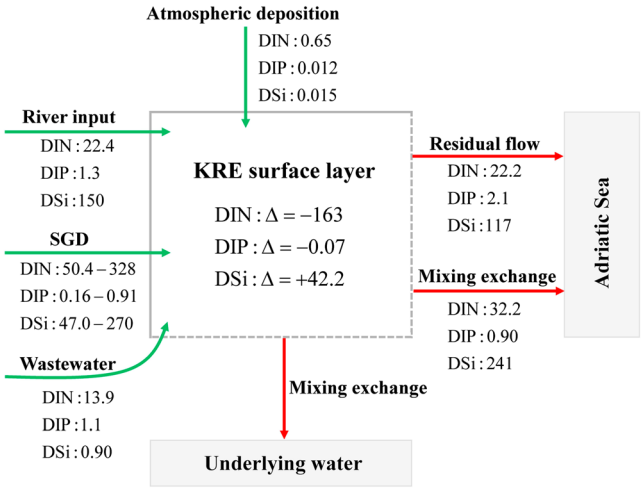

Figure 7. Nutrient budgets ($\times 10^3$ mol/day) in the KRE surface layer. The average SGD flux was used to calculate net SGD-derived nutrient fluxes and then to establish the total nutrient budgets.

Generally, the DIN:DIP ratios in groundwater are greater than the widely accepted average requirements of phytoplankton growth (16:1; Slomp & Van Cappellen, 2004). It was repeatedly observed that SGD-derived DIN:DIP ratios were much higher than DIN:DIP ratios in the rivers and other sources in coastal waters (Hwang et al., 2005; Lee et al., 2009; Waska & Kim, 2011). In this study, the average DIN:DIP ratio of net SGD-derived nutrients was approximately 320, which was much higher than those found in the KRE surface layer water (~17) and wastewater from the city of Šibenik (~12; Figure 7). Also, the DIN:DSi ratio in the groundwater was considerably different from that in the Krka River. However, DSi was not likely to be a limiting nutrient in those two water sources for the KRE. The DIN:DIP ratios in the surface water of the KRE ranged from 8 at TS station to 24 at KR4, with an average of 14 (Table 1), suggesting a potential lack of nitrogen. In comparison, DIN:DIP ratios in the groundwater were >100, which was notably unbalanced for the phytoplankton growth. Therefore, the submarine groundwater, which makes a substantial contribution to the KRE surface waters, has the potential to cause P-limitation of the microbial growth in the brackish part of the KRE water column. This situation can be compared to the case of the River Po, which pressures the northern Adriatic Sea by its high DIN:DIP ratio toward the P-limitation (Cozzi & Giani, 2011; Ivančić et al., 2016). We raise a note of caution when commenting DIN:DIP ratios in the surface productive waters that are close to Redfield's 16. Namely, surface waters are more complicated concerning the content and bioavailability of dissolved N and P in comparison to the deep nonproductive waters, with most N and P converted to nitrate and phosphate (Hrustić et al., 2017; Sarmiento & Gruber, 2006). The recent study has shown that the P-limitation in microbial communities may occur along with varying ratios (above and below 16) of balanced uptake of N and P (Hrustić et al., 2017). The supply of DIN, DIP, and DSi to the studied area through SGD was considerable for the overall nutrient budgets in the KRE. Moreover, SGD can play an important role in appearance of environmental problems in the KRE such as eutrophication (Legović et al., 1994), hypoxia (Cindrić et al., 2015; Legović et al., 1991), and phytoplankton bloom (Petricioli et al., 1996; Svensen et al., 2007). This is particularly critical in the Zaton Bay region, resulting in the frequent occurrence of phytoplankton bloom (Šupraha et al., 2014). Based on the example of KRE, SGD most likely plays a significant role for the nutrient budgets along the entire eastern coast of the Adriatic Sea where numerous karstic estuaries (Benac et al., 2003; Viličić et al., 2009) and marine lakes (Hrustić & Bobanović-Ćolić, 2017; Wunsam et al., 1999) are under the influence of SGD.

4.6. Net SGD-Derived DIC Flux Into the KRE Surface Layer

The total SGD-associated DIC flux into the KRE surface layer was $(0.77–4.40) \times 10^7$ mol/day, whereas the average DIC concentration in groundwater was 16.5 mmol/L. DIC flux from Krka River was 6.59×10^7 mol/day. Using the same method as for nutrient budgets, the net DIC flux derived from SGD was estimated to be $(0.37–2.17) \times 10^7$ mol/day, which accounted for 48–51% of the total SGD-associated DIC flux, and was equivalent to 5.6–33% of the concomitant DIC riverine inputs. These results suggested that SGD serves as an important DIC source to the KRE surface layer. Compared to other estuaries worldwide (Table 3), net SGD-derived DIC flux in this study was comparable to those reported for salt marshes/estuaries by Moore et al. (2006) and Porubsky et al. (2014), but much higher than those in other studies, indicating the high level DIC export via SGD in Krka River karstic estuary. Karst aquifers in the coastal Mediterranean Sea are common (Bakalowicz, 2018), and taking into account such a high transporting of DIC via SGD, these aquifers have the potential to contribute to ocean acidification (Doney et al., 2007; Flecha et al., 2015; Jeannin et al., 2016).

We further investigated karstic SGD-derived DIC by carrying out additional calculation here. The coastline surrounding the investigated part of the KRE surface layer is approximately 20.7 km long, and hence, an estimated net SGD-derived DIC flux can be calculated as $(1.78–10.4) \times 10^5$ mol · km · day. Based on the distribution of karst aquifers along the coasts worldwide (BGR, IAH, KIT & UNESCO , 2017), we estimated that the global coastlines of the karst aquifers are approximately 28,000 km long. Assuming uniformly distributed karst aquifers around the globe, which have similar DIC concentration in their groundwater, the global net SGD-derived DIC flux from karst aquifers would be $(0.18–1.06) \times 10^{13}$ mol/year. This number equals 8–48% of the DIC flux via SGD in the global mangrove ecosystem that has high DIC export rates and account for 2.7–9.6% of the global riverine DIC inputs (Chen et al., 2018; Maher et al., 2013). Just as reported in Chen et al. (2018), if the total SGD-derived DIC flux is used, then the estimated SGD-derived DIC flux in global karst aquifers along the coasts equals 17–97% of the flux in the global mangrove ecosystem. Therefore,

Table 3
Comparison of SGD-Derived DIC Fluxes in the Estuaries Worldwide

Region	SGD-derived DIC flux mol · m^2 · day	SGD-derived compared to river inputs %	Reference
Jiulong Estuary, China	0.12–0.90*	24–110	G. Z. Wang, Wang, et al. (2015)
Pearl River Estuary, China	0.30–0.69	33–77	Liu et al. (2018) and Liu et al. (2012)
Yarra River estuary, Australia	0.35	55	Santos et al. (2012)
Hat Head Estuary, Australia	0.69	na	Sadat-Noori et al. (2016)
Okatee Estuary, USA	1.96	na	Moore et al. (2006)
	1.08	na	Porubsky et al. (2014)
KRE surface layer, Croatia	0.40–2.34* (1.53)#	5.6–33(22)#	This study

*Net SGD-derived fluxes. #Values in brackets represent average value.
na: not available.

SGD from the DIC-enriched coastal karst aquifers is likely to be an important but easily ignored source for the carbon budget in the coastal seas worldwide. For these reasons, more robust researches should be conducted to provide more precise comparisons between the contributions of karst aquifers and mangrove systems to the DIC budget in the oceans.

The coastal karst aquifers are very vulnerable and sensitive to climate and environmental changes (Fleury et al., 2007). In general, SGD through submarine springs (fresh groundwater) in the coastal karst aquifer with saline water intrusion (recirculated groundwater) represents the conduit open to the sea. Therefore, the global climate change, especially sea level rise, will likely increase the contribution of the saline water intrusions into the coastal karst aquifers, resulting in more carbonate rocks dissolution, and production of more DIC, which then shall be transferred along with SGD flow into the coastal seas (Cao et al., 2016; Ketabchi et al., 2016). Consequently, the impact of net SGD-derived DIC associated with karst aquifers on the global carbon cycle shall become increasingly substantial. Therefore, robust and in-depth investigations related to this topic in the future are warranted.

5. Conclusion

In the highly stratified Krka River Estuary, we employed three methods including the three end-member mixing model, mass balance model, and time series observation over the full 24-hr tidal period to evaluate the contribution of SGD and derived nutrient fluxes into the water above the halocline. Even though the SGD accounted for only a small portion of the total water in the study area relative to the Krka River discharge and precipitation, net nutrient fluxes through SGD were important sources for the nutrient budgets in the KRE surface layer, especially for DIN and DSi. Additionally, nutrient-enriched SGD with high DIN: DIP ratios has a notable potential to impact the structure of the microbial community and productivity in the surface waters of the KRE and adjacent coastal sea. SGD-derived DIC should be included in carbon budgets of the coastal areas, especially because of the important effects of the sea level rise on the coastal karst dissolution as part of the current trend of global climate change. Eastern Adriatic could serve as a natural laboratory for more detailed studies on this topic because it is rich in stratified estuaries with numerous SGD embedded in the coastal system of karst. Seasonal and long-term studies in this area have great value to elucidate the significance of SGD-derived DIC for the carbon budgets of the coastal seas, and by using extrapolation, for carbon budgets of the oceans.

Acknowledgments
Financial support of the Croatian-Chinese Scientific and Technological Cooperation and Open Research Fund of State Key Laboratory of Estuarine and Costal Research (Grant SKLEC-KF201505), the Natural Science Foundation of China (Grants 41376089 and 41576083), and the Programme of Introducing Talents of Discipline to Universities (Grant B08022) are gratefully acknowledged. We thank all the colleagues in the field survey. We thank Nan Chiang (Harvard University, Massachusetts, USA) for proofreading and commenting on the manuscript. We also wish to thank Editor S. Bradley Moran, and two anonymous reviewers for their constructive comments for improvement of the original manuscript. All the data used for this study are available in Table 1 and supporting information file.

References

Ahel, M., Barlow, R. G., & Mantoura, R. (1996). Effect of salinity gradients on the distribution of phytoplankton pigments in a stratified estuary. *Marine Ecology Progress Series*, *143*, 289–295. http://doi.org/10.3354/meps143289

Ahel, M., & Terzić, S. (2003). Biogeochemistry of aromatic surfactants in microtidal estuaries. *CHIMIA International Journal for Chemistry*, *57*(9), 550–555. http://doi.org/10.2533/000942903777679019

Bakalowicz, M. (2018). Coastal karst groundwater in the Mediterranean: A resource to be preferably exploited onshore, not from karst submarine springs. *Geosciences*, *8*(7), 258. http://doi.org/10.3390/geosciences8070258

Baudron, P., Cockenpot, S., Lopez-Castejon, F., Radakovitch, O., Gilabert, J., Mayer, A., et al. (2015). Combining radon, short-lived radium isotopes and hydrodynamic modeling to assess submarine groundwater discharge from an anthropized semiarid watershed to a Mediterranean lagoon (Mar Menor, SE Spain). *Journal of Hydrology*, *525*, 55–71. http://doi.org/10.1016/j.jhydrol.2015.03.015

Benac, Č., Rubinić, J., & Ožanić, N. (2003). The origin and evolution of coastal and submarine springs in Bakar Bay. *Acta carsologica*, *32*(1), 157–171. http://doi.org/10.3986/ac.v32i1.371

Bejannin, S., vanBeek, P., Stieglitz, T., Souhaut, M., & Tamborski, J. (2017). Combining airbornethermal infrared images and radium isotopes to study submarine groundwater discharge along the French Mediterranean coastline. *Journal of Hydrology: Regional Studies*, *13*, 72–90. http://doi.org/10.1016/j.ejrh.2017.08.001

BGR, IAH, KIT & UNESCO (2017). World Karst Aquifer Map, 1: 40 000 000. Berlin, Reading, Karlsruhe and Paris.

Bituh, T., Petrinec, B., Marović, G., Senčar, J., & Gospodarić, I. (2008). ^{226}Ra and ^{228}Ra in Croatian Rivers. *Collegium antropologicum*, *32*(2), 105–108.

Bonacci, O. (1995). Ground water behaviour in karst: Example of the Ombla Spring (Croatia). *Journal of Hydrology*, *165*(1-4), 113–134. http://doi.org/10.1016/0022-1694(94)02577-X

Bonacci, O., Jukić, D., & Ljubenkov, I. (2006). Definition of catchment area in karst: Case of the rivers Krčić and Krka, Croatia. *Hydrological Sciences Journal*, *51*(4), 682–699. http://doi.org/10.1623/hysj.51.4.682

Burnett, W. C., Aggarwal, P. K., Aureli, A., Bokuniewicz, H., Cable, J. E., Charette, M. A., et al. (2006). Quantifying submarine groundwater discharge in the coastal zone via multiple methods. *Science of the Total Environment*, *367*(2-3), 498–543. http://doi.org/10.1016/j.scitotenv.2006.05.009

Burnett, W. C., Bokuniewicz, H., Huettel, M., Moore, W. S., & Taniguchi, M. (2003). Groundwater and pore water inputs to the coastal zone. *Biogeochemistry*, *66*(1/2), 3–33. http://doi.org/10.1023/B:Biog.0000006066.21240.53

Burnett, W. C., & Dulaiova, H. (2006). Radon as a tracer of submarine groundwater discharge into a boat basin in Donnalucata, Sicily. *Continental Shelf Research*, *26*(7), 862–873. http://doi.org/10.1016/j.csr.2005.12.003

Cai, W.-J., Dai, M., Wang, Y., Zhai, W., Huang, T., Chen, S., et al. (2004). The biogeochemistry of inorganic carbon and nutrients in the Pearl River estuary and the adjacent Northern South China Sea. *Continental Shelf Research*, *24*(12), 1301–1319. http://doi.org/10.1016/j.csr.2004.04.005

Cao, J., Hu, B., Groves, C., Huang, F., Yang, H., & Zhang, C. (2016). Karst dynamic system and the carbon cycle. *Zeitschrift für Geomorphologie, Supplementary Issues*, *60*(2), 35–55. http://doi.org/10.1127/zfg_suppl/2016/00304

Cauwet, G. (1991). Carbon inputs and biogeochemical processes at the halocline in a stratified estuary: Krka River, Yugoslavia. *Marine Chemistry*, *32*(2-4), 269–283. http://doi.org/10.1016/0304-4203(91)90043-V

Cerdà-Domènech, M., Rodellas, V., Folch, A., & Garcia-Orellana, J. (2017). Constraining the temporal variations of Ra isotopes and Rn in the groundwater end-member: Implications for derived SGD estimates. *Science of the Total Environment*, *595*, 849–857. https://doi.org/10.1016/j.scitotenv.2017.03.005

Cetinić, I., Viličić, D., Burić, Z., & Olujić, G. (2006). Phytoplankton seasonality in a highly stratified karstic estuary (Krka, Adriatic Sea). *Hydrobiologia*, *555*(1), 31–40. https://doi.org/10.1007/s10750-005-1103-7

Chen, X., Zhang, F., Lao, Y., Wang, X., Du, J., & Santos, I. R. (2018). Submarine groundwater discharge-derived carbon fluxes in mangroves: An important component of blue carbon budgets? *Journal of Geophysical Research: Oceans*, *123*, 6962–6979. http://doi.org/10.1029/2018JC014448

Cindrić, A. M., Garnier, C., Oursel, B., Pizeta, I., & Omanovic, D. (2015). Evidencing the natural and anthropogenic processes controlling trace metals dynamic in a highly stratified estuary: The Krka River Estuary (Adriatic, Croatia). *Marine Pollution Bulletin*, *94*(1-2), 199–216. http://doi.org/10.1016/j.marpolbul.2015.02.029

Cota, G., Pomeroy, L., Harrison, W., Jones, E., Peters, F., Sheldon, W. Jr., & Weingartner, T. R. (1996). Nutrients, primary production and microbial heterotrophy in the southeastern Chukchi Sea: Arctic summer nutrient depletion and heterotrophy. *Marine Ecology Progress Series*, *135*, 247–258. http://doi.org/10.3354/meps135247

Cozzi, S., & Giani, M. (2011). River water and nutrient discharges in the Northern Adriatic Sea: Current importance and long term changes. *Continental Shelf Research*, *31*(18), 1881–1893. https://doi.org/10.1016/j.csr.2011.08.010

Cukrov, N., & Barišić, D. (2006). Spatial distribution of 40 K and ^{232}Th in recent sediments of the Krka River Estuary. *Croatica Chemica Acta*, *79*(1), 115–118.

Cukrov, N., Cmuk, P., Mlakar, M., & Omanović, D. (2008). Spatial distribution of trace metals in the Krka River, Croatia: An example of the self-purification. *Chemosphere*, *72*(10), 1559–1566. http://doi.org/10.1016/j.chemosphere.2008.04.038

Cukrov, N., Mlakar, M., Cuculić, V., & Barićić, D. (2009). Origin and transport of ^{238}U and ^{226}Ra in riverine, estuarine and marine sediments of the Krka River, Croatia. *Journal of Environmental Radioactivity*, *100*(6), 497–504. http://doi.org/10.1016/j.jenvrad.2009.03.012

Cukrov, N., Tepić, N., Omanović, D., Lojen, S., Bura-Nakić, E., Vojvodić, V., & Pižeta, I. (2012). Qualitative interpretation of physico-chemical and isotopic parameters in the Krka River (Croatia) assessed by multivariate statistical analysis. *International Journal of Environmental Analytical Chemistry*, *92*(10), 1187–1199. http://doi.org/10.1080/03067319.2010.550003

Denant, V., Saliot, A., & Mantoura, R. (1991). Distribution of algal chlorophyll and carotenoid pigments in a stratified estuary: The Krka River, Adriatic Sea. *Marine Chemistry*, *32*(2-4), 285–297. http://doi.org/10.1016/0304-4203(91)90044-W

Doney, S. C., Mahowald, N., Lima, I., Feely, R. A., Mackenzie, F. T., Lamarque, J.-F., & Rasch, P. J. (2007). Impact of anthropogenic atmospheric nitrogen and sulfur deposition on ocean acidification and the inorganic carbon system. *Proceedings of the National Academy of Sciences*, *104*(37), 14,580–14,585. http://doi.org/10.1073/pnas.0702218104

El-Gamal, A. A., Peterson, R. N., & Burnett, W. C. (2012). Detecting freshwater inputs via groundwater discharge to Marina Lagoon, Mediterranean Coast, Egypt. *Estuaries and Coasts*, *35*(6), 1486–1499. http://doi.org/10.1007/s12237-012-9539-2

Flecha, S., Pérez, F. F., García-Lafuente, J., Sammartino, S., Ríos, A. F., & Huertas, I. E. (2015). Trends of pH decrease in the Mediterranean Sea through high frequency observational data: Indication of ocean acidification in the basin. *Scientific Reports*, *5*(1), 16770. http://doi.org/10.1038/srep16770

Fleury, P., Bakalowicz, M., & de Marsily, G. (2007). Submarine springs and coastal karst aquifers: A review. *Journal of Hydrology*, *339*(1-2), 79–92. http://doi.org/10.1016/j.jhydrol.2007.03.009

Fuks, D., Devescovi, M., Precali, R., Krstulović, N., & Šolić, M. (1991). Bacterial abundance and activity in the highly stratified estuary of the Krka River. *Marine Chemistry*, *32*(2-4), 333–346. http://doi.org/10.1016/0304-4203(91)90047-Z

Garcia-Orellana, J., Cochran, J. K., Bokuniewicz, H., Yang, S., & Beck, A. J. (2010). Time-series sampling of ^{223}Ra and ^{224}Ra at the inlet to Great South Bay (New York): A strategy for characterizing the dominant terms in the Ra budget of the bay. *Journal of Environmental Radioactivity*, *101*(7), 582–588. http://doi.org/10.1016/j.jenvrad.2009.12.005

Garcia-Solsona, E., Garcia-Orellana, J., Masqué, P., Garces, E., Radakovitch, O., Mayer, A., et al. (2010). An assessment of karstic submarine groundwater and associated nutrient discharge to a Mediterranean coastal area (Balearic Islands, Spain) using radium isotopes. *Biogeochemistry*, *97*(2-3), 211–229. http://doi.org/10.1007/s10533-009-9368-y

Garcia-Solsona, E., Garcia-Orellana, J., Masqué, P., Rodellas, V., Mejias, M., Ballesteros, B., & Domínguez, J. A. (2010). Groundwater and nutrient discharge through karstic coastal springs (Castelló, Spain). *Biogeosciences*, *7*(9), 2625–2638. http://doi.org/10.5194/bg-7-2625-2010

Gonneea, M. E., Charette, M. A., Liu, Q., Herrera-Silveira, J. A., & Morales-Ojeda, S. M. (2014). Trace element geochemistry of groundwater in a karst subterranean estuary (Yucatan Peninsula, Mexico). *Geochimica et Cosmochimica Acta*, *132*, 31–49. http://doi.org/10.1016/j.gca.2014.01.037

Gordon, D. C., Boudreau, P., Mann, K., Ong, J., Silvert, W., Smith, S., et al. (1996). *LOICZ biogeochemical modelling guidelines, LOICZ Core Project*. Yerseke: Netherlands Institute for Sea Research.

Grasshoff, K., Kremling, K., & Ehrhardt, M. (2009). *Methods of seawater analysis*. New York: John Wiley & Sons.

Gržetić, Z., Precali, R., Degobbis, D., & Škrivanić, A. (1991). Nutrient enrichment and phytoplankton response in an Adriatic karstic estuary. *Marine Chemistry*, *32*(2-4), 313–331. http://doi.org/10.1016/0304-4203(91)90046-Y

Gu, H., Moore, W. S., Zhang, L., Du, J., & Zhang, J. (2012). Using radium isotopes to estimate the residence time and the contribution of submarine groundwater discharge (SGD) in the Changjiang effluent plume, East China Sea. *Continental Shelf Research*, *35*, 95–107. http://doi.org/10.1016/j.csr.2012.01.002

Gunes, K., Tuncsiper, B., Ayaz, S., & Drizo, A. (2012). The ability of free water surface constructed wetland system to treat high strength domestic wastewater: A case study for the Mediterranean. *Ecological Engineering*, *44*, 278–284. http://doi.org/10.1016/j.ecoleng.2012.04.008

Hatje, V., Apte, S. C., Hales, L. T., & Birch, G. F. (2003). Dissolved trace metal distributions in Port Jackson estuary (Sydney Harbour), Australia. *Marine Pollution Bulletin*, *46*(6), 719–730. http://doi.org/10.1016/s0025-326x(03)00061-4

Hrustić, E., & Bobanović-Ćolić, S. (2017). Hypoxia in deep waters of moderately eutrophic marine lakes, Island of Mljet, eastern Adriatic Sea. *Scientia Marina*, *81*(4), 431–447. http://doi.org/10.3989/scimar.04523.25A

Hrustić, E., Lignell, R., Riebesell, U., & Thingstad, T. F. (2017). Exploring the distance between nitrogen and phosphorus limitation in mesotrophic surface waters using a sensitive bioassay. *Biogeosciences*, *14*(2), 379–387. http://doi.org/10.5194/bg-14-379-2017

Hwang, D.-W., Kim, G., Lee, Y.-W., & Yang, H.-S. (2005). Estimating submarine inputs of groundwater and nutrients to a coastal bay using radium isotopes. *Marine Chemistry*, *96*(1-2), 61–71. http://doi.org/10.1016/j.marchem.2004.11.002

Ivančić, I., & Degobbis, D. (1984). An optimal manual procedure for ammonia analysis in natural waters by the indophenol blue method. *Water Research*, *18*(9), 1143–1147. http://doi.org/10.1016/0043-1354(84)90230-6

Ivančić, I., Pfannkuchen, M., Godrijan, J., Djakovac, T., Pfannkuchen, D. M., Korlević, M., et al. (2016). Alkaline phosphatase activity related to phosphorus stress of microphytoplankton in different trophic conditions. *Progress in Oceanography*, *146*, 175–186. http://doi.org/10.1016/j.pocean.2016.07.003

Jeannin, P.-Y., Hessenauer, M., Malard, A., & Chapuis, V. (2016). Impact of global change on karst groundwater mineralization in the Jura Mountains. *Science of the Total Environment*, *541*, 1208–1221. http://doi.org/10.1016/j.scitotenv.2015.10.008

Ji, T., Du, J., Moore, W. S., Zhang, G., Su, N., & Zhang, J. (2013). Nutrient inputs to a lagoon through submarine groundwater discharge: The case of Laoye Lagoon, Hainan, China. *Journal of Marine Systems*, *111-112*, 253–262. http://doi.org/10.1016/j.jmarsys.2012.11.007

Kelly, R. P., & Moran, S. B. (2002). Seasonal changes in groundwater input to a well-mixed estuary estimated using radium isotopes and implications for coastal nutrient budgets. *Limnology and Oceanography*, *47*(6), 1796–1807. http://doi.org/10.4319/lo.2002.47.6.1796

Ketabchi, H., Mahmoodzadeh, D., Ataie-Ashtiani, B., & Simmons, C. T. (2016). Sea-level rise impacts on seawater intrusion in coastal aquifers: Review and integration. *Journal of Hydrology*, *535*, 235–255. http://doi.org/10.1016/j.jhydrol.2016.01.083

Kniewald, G., Marguš, D., & Mihelčić, G. (2006), Formation of the Krka River Estuary in Croatia and the travertine barrier phenomenon, paper presented at Fluxes of Small and Medium-size Mediterranean Rivers: Impact on Coastal Areas. CIESM Workshop Monographs.

Krest, J. M., & Moore, W. S. (1999). ^{226}Ra and ^{228}Ra in the mixing zones of the Mississippi and Atchafalaya Rivers: Indicators of groundwater input. *Marine Chemistry*, *64*(3), 129–152. http://doi.org/10.1016/S0304-4203(98)00070-X

Kwokal, Z., Frančišković-Bilinski, S., Bilinski, H., & Branica, M. (2002). A comparison of anthropogenic mercury pollution in Kaštela Bay (Croatia) with pristine estuaries in Ore (Sweden) and Krka (Croatia). *Marine Pollution Bulletin*, *44*(10), 1152–1157. https://doi.org/10.1016/S0025-326X(02)00134-0

Lee, Y. W., Hwang, D. W., Kim, G., Lee, W. C., & Oh, H. T. (2009). Nutrient inputs from submarine groundwater discharge (SGD) in Masan Bay, an embayment surrounded by heavily industrialized cities, Korea. *Science of the Total Environment*, *407*(9), 3181–3188. http://doi.org/10.1016/j.scitotenv.2008.04.013

Legović, T. (1991). Exchange of water in a stratified estuary with an application to Krka (Adriatic Sea). *Marine Chemistry*, *32*(2-4), 121–135. http://doi.org/10.1016/0304-4203(91)90032-R

Legović, T., Petricioli, D., & Žutić, V. (1991). Hypoxia in a pristine stratified estuary (Krka, Adriatic Sea). *Marine Chemistry*, *32*(2-4), 347–359. http://doi.org/10.1016/0304-4203(91)90048-2

Legović, T., Žutić, V., Gržetić, Z., Cauwet, G., Precali, R., & Viličić, D. (1994). Eutrophication in the Krka estuary. *Marine Chemistry*, *46*(1-2), 203–215. http://doi.org/10.1016/0304-4203(94)90056-6

Li, L., Barry, D. A., Stagnitti, F., & Parlange, J. Y. (1999). Submarine groundwater discharge and associated chemical input to a coastal sea. *Water Resources Research*, *35*(11), 3253–3259. http://doi.org/10.1029/1999WR900189

Liu, J., Du, J., Wu, Y., & Liu, S. (2018). Nutrient input through submarine groundwater discharge in two major Chinese estuaries: The Pearl River Estuary and the Changjiang River Estuary. *Estuarine, Coastal and Shelf Science*, *203*, 17–28. http://doi.org/10.1016/j.ecss.2018.02.005

Liu, J., Du, J., & Yi, L. (2017). Ra tracer-based study of submarine groundwater discharge and associated nutrient fluxes into the Bohai Sea, China: A highly human-affected marginal sea. *Journal of Geophysical Research: Oceans*, *122*, 8646–8660. http://doi.org/10.1002/2017JC013095

Liu, Q., Dai, M., Chen, W., Huh, C. A., Wang, G., Li, Q., & Charette, M. A. (2012). How significant is submarine groundwater discharge and its associated dissolved inorganic carbon in a river-dominated shelf system? *Biogeosciences*, *9*(5), 1777–1795. http://doi.org/10.5194/bg-9-1777-2012

Liu, S. M., Hong, G. H., Zhang, J., Ye, X. W., & Jiang, X. L. (2009). Nutrient budgets for large Chinese estuaries. *Biogeosciences*, *6*(10), 2245–2263. http://doi.org/10.5194/bg-6-2245-2009

Liu, S. M., Li, R. H., Zhang, G. L., Wang, D. R., Du, J. Z., Herbeck, L. S., et al. (2011). The impact of anthropogenic: Activities on nutrient dynamics in the tropical Wenchanghe and Wenjiaohe Estuary and Lagoon system in East Hainan, China. *Marine Chemistry*, *125*(1-4), 49–68. http://doi.org/10.1016/j.marchem.2011.02.003

Maher, D. T., Santos, I. R., Golsby-Smith, L., Gleeson, J., & Eyre, B. D. (2013). Groundwater-derived dissolved inorganic and organic carbon exports from a mangrove tidal creek: The missing mangrove carbon sink? *Limnology and Oceanography*, *58*(2), 475–488. http://doi.org/10.4319/lo.2013.58.2.0475

Markaki, Z., Loÿe-Pilot, M. D., Violaki, K., Benyahya, L., & Mihalopoulos, N. (2010). Variability of atmospheric deposition of dissolved nitrogen and phosphorus in the Mediterranean and possible link to the anomalous seawater N/P ratio. *Marine Chemistry*, *120*(1-4), 187–194. http://doi.org/10.1016/j.marchem.2008.10.005

McCormack, T., Gill, L., Naughton, O., & Johnston, P. (2014). Quantification of submarine/intertidal groundwater discharge and nutrient loading from a lowland karst catchment. *Journal of Hydrology*, *519*, 2318–2330. http://doi.org/10.1016/j.jhydrol.2014.09.086

McCoy, C., Viso, R., Peterson, R. N., Libes, S., Lewis, B., Ledoux, J., et al. (2011). Radon as an indicator of limited cross-shelf mixing of submarine groundwater discharge along an open ocean beach in the South Atlantic Bight during observed hypoxia. *Continental Shelf Research*, *31*(12), 1306–1317. http://doi.org/10.1016/j.csr.2011.05.009

Moore, W. S. (1996). Large groundwater inputs to coastal waters revealed by ^{226}Ra enrichments. *Nature Geoscience*, *380*(6575), 612–614. http://doi.org/10.1038/380612a0

Moore, W. S. (2003). Sources and fluxes of submarine groundwater discharge delineated by radium isotopes. *Biogeochemistry*, *66*(1/2), 75–93. http://doi.org/10.1023/B:BIOG.0000006065.77764.a0

Moore, W. S. (2006). Radium isotopes as tracers of submarine groundwater discharge in Sicily. *Continental Shelf Research*, *26*(7), 852–861. http://doi.org/10.1016/j.csr.2005.12.004

Moore, W. S. (2010). The effect of submarine groundwater discharge on the ocean. *Annual Review of Marine Science*, *2*(1), 59–88. http://doi.org/10.1146/annurev-marine-120308-081019

Moore, W. S., Blanton, J. O., & Joye, S. B. (2006). Estimates of flushing times, submarine groundwater discharge, and nutrient fluxes to Okatee Estuary, South Carolina. *Journal of Geophysical Research*, *111*, C09006. http://doi.org/10.1029/2005JC003041

Moore, W. S., Sarmiento, J. L., & Key, R. M. (2008). Submarine groundwater discharge revealed by ^{228}Ra distribution in the upper Atlantic Ocean. *Nature Geoscience*, *1*(5), 309–311. http://doi.org/10.1038/ngeo183

Ollivier, P., Claude, C., Radakovitch, O., & Hamelin, B. (2008). TIMS measurements of ^{226}Ra and ^{228}Ra in the Gulf of Lion, an attempt to quantify submarine groundwater discharge. *Marine Chemistry*, *109*(3-4), 337–354. http://doi.org/10.1016/j.marchem.2007.08.006

Pavlidou, A., Papadopoulos, V. P., Hatzianestis, I., Simboura, N., Patiris, D., & Tsabaris, C. (2014). Chemical inputs from a karstic submarine groundwater discharge (SGD) into an oligotrophic Mediterranean coastal area. *Science of the Total Environment*, *488-489*, 1–13. http://doi.org/10.1016/j.scitotenv.2014.04.056

Peterson, R. N., Burnett, W. C., Taniguchi, M., Chen, J., Santos, I. R., & Ishitobi, T. (2008). Radon and radium isotope assessment of submarine groundwater discharge in the Yellow River delta, China. *Journal of Geophysical Research*, *113*, C09021. http://doi.org/10.1029/2008JC004776

Petricioli, D., BakranPetricioli, T., Viličić, D., & Požar-Domac, A. (1996). Freshwater phytoplankton bloom in Visovac lake—A possible cause of benthic mortality in Krka estuary (Adriatic sea, Croatia). *Marine Ecology*, *17*(1-3), 373–382. http://doi.org/10.1111/j.1439-0485.1996.tb00515.x

Porubsky, W. P., Weston, N. B., Moore, W. S., Ruppel, C., & Joye, S. B. (2014). Dynamics of submarine groundwater discharge and associated fluxes of dissolved nutrients, carbon, and trace gases to the coastal zone (Okatee River estuary, South Carolina). *Geochimica et Cosmochimica Acta*, *131*, 81–97. http://doi.org/10.1016/j.gca.2013.12.030

Powley, H. R., Durr, H. H., Lima, A. T., Krom, M. D., & Van Cappellen, P. (2016). Direct discharges of domestic wastewater are a major source of phosphorus and nitrogen to the Mediterranean Sea. *Environmental Science & Technology*, *50*(16), 8722–8730. http://doi.org/10.1021/acs.est.6b01742

Rapaglia, J., Ferrarin, C., Zaggia, L., Moore, W. S., Umgiesser, G., Garcia-Solsona, E., et al. (2010). Investigation of residence time and groundwater flux in Venice Lagoon: Comparing radium isotope and hydrodynamic models. *Journal of Environmental Radioactivity*, *101*(7), 571–581. http://doi.org/10.1016/j.jenvrad.2009.08.010

Rapaglia, J., Koukoulas, S., Zaggia, L., Lichter, M., Manfé, G., & Vafeidis, A. T. (2012). Quantification of submarine groundwater discharge and optimal radium sampling distribution in the Lesina Lagoon, Italy. *Journal of Marine Systems*, *91*(1), 11–19. http://doi.org/10.1016/j.jmarsys.2011.09.003

Redfield, A. C. (1963). The influence of organisms on the composition of seawater. *The Sea*, *2*, 26–77.

Rengarajan, R., & Sarma, V. V. S. S. (2015). Submarine groundwater discharge and nutrient addition to the coastal zone of the Godavari estuary. *Marine Chemistry*, *172*, 57–69. http://doi.org/10.1016/j.marchem.2015.03.008

Rodellas, V., Garcia-Orellana, J., Masque, P., Feldman, M., & Weinstein, Y. (2015). Submarine groundwater discharge as a major source of nutrients to the Mediterranean Sea. *Proceedings of the National Academy of Sciences*, *112*(13), 3926–3930. http://doi.org/10.1073/pnas.1419049112

Rodellas, V., Garcia-Orellana, J., Tovar-Sánchez, A., Basterretxea, G., López-Garcia, J. M., Sánchez-Quiles, D., et al. (2014). Submarine groundwater discharge as a source of nutrients and trace metals in a Mediterranean bay (Palma Beach, Balearic Islands). *Marine Chemistry*, *160*, 56–66. http://doi.org/10.1016/j.marchem.2014.01.007

Rodellas, V., Garcia-Orellana, J., Trezzi, G., Masqué, P., Stieglitz, T. C., Bokuniewicz, H., et al. (2017). Using the radium quartet to quantify submarine groundwater discharge and porewater exchange. *Geochimica et Cosmochimica Acta*, *196*, 58–73. https://doi.org/10.1016/j.gca.2016.09.016

Sadat-Noori, M., Maher, D. T., & Santos, I. R. (2016). Groundwater discharge as a source of dissolved carbon and greenhouse gases in a subtropical estuary. *Estuaries and Coasts*, *39*(3), 639–656. http://doi.org/10.1007/s12237-015-0042-4

Sadat-Noori, M., Santos, I. R., Sanders, C. J., Sanders, L. M., & Maher, D. T. (2015). Groundwater discharge into an estuary using spatially distributed radon time series and radium isotopes. *Journal of Hydrology*, *528*, 703–719. http://doi.org/10.1016/j.jhydrol.2015.06.056

Sanford, L. P., Boicourt, W. C., & Rives, S. R. (1992). Model for estimating tidal flushing of small embayments. *Journal of Waterway, Port, Coastal and Ocean Engineering*, *118*(6), 635–654. https://doi.org/10.1061/(ASCE)0733-950X(1992)118:6(635)

Santos, I. R., Cook, P. L., Rogers, L., De Weys, J., & Eyre, B. D. (2012). The "salt wedge pump": Convection-driven pore-water exchange as a source of dissolved organic and inorganic carbon and nitrogen to an estuary. *Limnology and Oceanography*, *57*(5), 1415–1426. http://doi.org/10.4319/lo.2012.57.5.1415

Sarmiento, J. L., & Gruber, N. (2006). *Ocean biogeochemical dynamics*, (pp. 1–191). Princeton and Oxford: Princeton University Press.

Slomp, C. P., & Van Cappellen, P. (2004). Nutrient inputs to the coastal ocean through submarine groundwater discharge: Controls and potential impact. *Journal of Hydrology*, *295*(1-4), 64–86. http://doi.org/10.1016/j.jhydrol.2004.02.018

Stieglitz, T. C., van Beek, P., Souhaut, M., & Cook, P. G. (2013). Karstic groundwater discharge and seawater recirculation through sediments in shallow coastal Mediterranean lagoons, determined from water, salt and radon budgets. *Marine Chemistry*, *156*, 73–84. http://doi.org/10.1016/j.marchem.2013.05.005

Strickland, J. D., & Parsons, T. R. (1972). *A practical handbook of seawater analysis*, (2nd ed.). Ottawa: Bulletin of the Fisheries Research Board of Canada.

Su, N., Du, J., Duan, Z., Deng, B., & Zhang, J. (2015). Radium isotopes and their environmental implications in the Changjiang River system. *Estuarine, Coastal and Shelf Science*, *156*, 155–164. http://doi.org/10.1016/j.ecss.2014.12.017

Su, N., Du, J., Moore, W. S., Liu, S., & Zhang, J. (2011). An examination of groundwater discharge and the associated nutrient fluxes into the estuaries of eastern Hainan Island, China using 226Ra. *Science of the Total Environment*, *409*(19), 3909–3918. http://doi.org/10.1016/j.scitotenv.2011.06.017

Šupraha, L., Bosak, S., Ljubešić, Z., Mihanović, H., Olujić, G., Mikac, I., & Viličić, D. (2014). Cryptophyte bloom in a Mediterranean estuary: High abundance of Plagioselmis of prolonga in the Krka River Estuary (eastern Adriatic Sea). *Scientia Marina*, *78*(3), 329–338. http://doi.org/10.3989/scimar.03998.28C

Svensen, C., Viličić, D., Wassmann, P., Arashkevich, E., & Ratkova, T. (2007). Plankton distribution and vertical flux of biogenic matter during high summer stratification in the Krka estuary (Eastern Adriatic). *Estuarine, Coastal and Shelf Science*, *71*(3-4), 381–390. http://doi.org/10.1016/j.ecss.2006.07.022

Swarzenski, P., Burnett, W., Greenwood, W., Herut, B., Peterson, R., Dimova, N., et al. (2006). Combined time-series resistivity and geochemical tracer techniques to examine submarine groundwater discharge at Dor Beach, Israel. *Geophysical Research Letters*, *33*, L24405. http://doi.org/10.1029/2006GL028282

Tamborski, J., Bejannin, S., Garcia-Orellana, J., Souhaut, M., Charbonnier, C., Anschutz, P., et al. (2018). A comparison between water circulation and terrestrially-driven dissolved silica fluxes to the Mediterranean Sea traced using radium isotopes. *Geochimica et Cosmochimica Acta*, *238*, 496–515. http://doi.org/10.1016/j.gca.2018.07.022

Viličić, D., Kuzmić, M., Bosak, S., Šilović, T., Hrustić, E., & Burić, Z. (2009). Distribution of phytoplankton along the thermohaline gradient in the north-eastern Adriatic channel; winter aspect. *Oceanologia*, *51*(4), 495–513. https://doi.org/10.5697/oc.51-4.495

Viličić, D., Legović, T., & Žutić, V. (1989). Vertical distribution of phytoplankton in a stratified estuary. *Aquatic Sciences*, *51*(1), 31–46. https://doi.org/10.1007/BF00877779

Wang, G. Z., Wang, Z. Y., Zhai, W. D., Moore, W. S., Li, Q., Yan, X. L., et al. (2015). Net subterranean estuarine export fluxes of dissolved inorganic C, N, P, Si, and total alkalinity into the Jiulong River estuary, China. *Geochimica et Cosmochimica Acta*, *149*, 103–114. http://doi.org/10.1016/j.gca.2014.11.001

Wang, X., Baskaran, M., Su, K., & Du, J. (2018). The important role of submarine groundwater discharge (SGD) to derive nutrient fluxes into river dominated ocean margins—The East China Sea. *Marine Chemistry*, *204*, 121–132. http://doi.org/10.1016/j.marchem.2018.05.010

Wang, X., & Du, J. (2016). Submarine groundwater discharge into typical tropical lagoons: A case study in eastern Hainan Island, China. *Geochemistry, Geophysics, Geosystems*, *17*, 4366–4382. http://doi.org/10.1002/2016GC006502

Wang, X., Du, J., Ji, T., Wen, T., Liu, S., & Zhang, J. (2014). An estimation of nutrient fluxes via submarine groundwater discharge into the Sanggou Bay—A typical multi-species culture ecosystem in China. *Marine Chemistry*, *167*, 113–122. http://doi.org/10.1016/j.marchem.2014.07.002

Wang, X., Li, H., Jiao, J. J., Barry, D. A., Li, L., Luo, X., et al. (2015). Submarine fresh groundwater discharge into Laizhou Bay comparable to the Yellow River flux. *Science Reports*, *5*(1). http://doi.org/10.1038/srep08814

Waska, H., & Kim, G. (2011). Submarine groundwater discharge (SGD) as a main nutrient source for benthic and water-column primary production in a large intertidal environment of the Yellow Sea. *Journal of Sea Research*, *65*(1), 103–113. http://doi.org/10.1016/j.seares.2010.08.001

Wunsam, S., Schmidt, R., & Müller, J. (1999). Holocene lake development of two Dalmatian lagoons (Malo and Veliko Jezero, Isle of Mljet) in respect to changes in Adriatic sea level and climate. *Palaeogeography, Palaeoclimatology, Palaeoecology*, *146*(1-4), 251–281. http://doi.org/10.1016/S0031-0182(98)00147-3

Zavatarelli, M., Raicich, F., Bregant, D., Russo, A., & Artegiani, A. (1998). Climatological biogeochemical characteristics of the Adriatic Sea. *Journal of Marine Systems*, *18*(1-3), 227–263. http://doi.org/10.1016/S0924-7963(98)00014-1

Žic, V., & Branica, M. (2006). Iodate and iodide distributions in the waters of a stratified estuary. *Croatica Chemica Acta*, *79*(1), 143–153.

Žutic, V., & Legović, T. (1987). A film of organic matter at the fresh-water/sea-water interface of an estuary. *Nature*, *328*(6131), 612–614. https://doi.org/10.1038/328612a0